Bonding and magnetism of chemisorbed oxygen on Fe(001)

Hong Huang and J. Hermanson

Department of Physics, Montana State University, Bozeman, Montana 59717

(Received 25 February 1985)

The electronic structure and magnetism of 1×1 O/Fe(001) was studied by the self-consistent localized-orbital (SCLO) method. A five-layer Fe(001) substrate was adopted in which the first interplanar spacing was 7.5% expanded compared with the bulk spacing. Oxygen atoms filled the fourfold hollow sites on both sides of the slab, with an Fe-O interplanar spacing of 0.48 Å. This interface geometry was determined in a previous low-energy-electron-diffraction (LEED) analysis. We find that the oxygen atoms have significant bonding to both the surface and subsurface Fe layers. "Horizontal" bonding (within the surface plane) is primarily due to the planar orbitals $3d_{xy}$ and $3d_{x^2-y^2}$ on Fe atoms, and $2p_x$ and $2p_y$ orbitals on oxygen. "Vertical" bonding of oxygen to subsurface iron is accomplished through Fe $3d_{z^2}$ and O $2p_z$ orbitals. Oxygenlike energy bands were obtained 4 to 8 eV below the Fermi energy E_F, with exchange splittings of 0.5 to 1.0 eV. The oxygen adlayer has a magnetic moment of $0.24\mu_B$ per atom, while surface Fe atoms have a moment of $2.93\mu_B$, essentially unchanged from the clean-surface value $2.89\mu_B$. Oxygen atoms have a net charge of 0.6 electron drawn from the surface and subsurface iron planes; as a result the work function increases 1.4 eV compared with the clean substrate, in disagreement with measurements on O/Fe(001), which obtain much smaller shifts. The discrepancy may be due to absorption of oxygen into the metal.

I. INTRODUCTION

Oxygen chemisorption on metal surfaces furnishes a prototypical model of a strong surface bond. Due to the large electronegativity of oxygen, substantial charge transfer from the metal surface to the adsorbate is expected. According to a recent LEED structure analysis,[1] the Fe(001) surface develops full monolayer coverage of oxygen, in 1×1 geometry, at about 5 L exposure (1 L = 1 langmuir $= 10^{-6}$ Torr sec). The Fe-O interlayer distance was inferred to be 0.48 Å, with oxygen atoms occupying the fourfold hollow sites in close proximity to subsurface Fe atoms. The first Fe-Fe interlayer spacing is apparently expanded by 7.5% compared with the bulk metal. In this work as well as a subsequent electron-energy-loss-spectroscopy (EELS) study,[2] the $c(2 \times 2)$ O/Fe(001) structure reported by other groups[3,4] could not be reproduced.

The electronic structure of the O/Fe(001) system has been studied[4] using ultraviolet photoemission spectroscopy (UPS). An oxygen-induced level centered 5.5 eV below E_F was observed for exposures below 1.5 L, while the Fe d-band emission was almost unaffected by the adsorption. For larger oxygen exposures, the 5.5-eV peak broadened substantially, and the d-band emission was attenuated; at 60 L the photoelectron energy distribution was very similar to that of FeO. During the adsorption, the LEED pattern changed from 1×1 (at 0 L) to $c(2 \times 2)$ at 1.5 L, returning to 1×1 at 4 L. This behavior differs from that observed in the recent LEED structure analysis,[1] where oxygen exposure caused no changes in the geometry of the 1×1 LEED pattern, but did cause changes in intensities of the diffracted beams. Auger spectra[1] suggest that the full monolayer stage is reached

at 6 L. UPS data on polycrystalline Fe films[5] also contain a 5.5-eV oxygen peak which broadens and intensifies with increasing coverage.

Recently, oxygen chemisorption and the initial oxidation of Fe(001) was studied using EELS combined with LEED, Auger-electron and secondary-electron-emission spectroscopies, and work-function-change measurements.[2] Three stages of oxygen bonding were identified: (1) dissociative chemisorption below 3 L, (2) oxygen incorporation into the selvedge region between 3 and 20 L, and (3) oxidation above 20 L, leading to the formation of γ-Fe_2O_3. The exact nature and extent of the oxygen incorporation is not known, although it influences both LEED and UPS analyses. An EELS peak ascribed to a bonding-antibonding electronic transition within the adlayer was observed[2] at 6 eV below 3 L.

A few electronic structure calculations have been performed using cluster models of the O/Fe(001) chemisorption system.[6-8] In spin-polarized computations for the cluster O/Fe$_5$, Anderson[6] obtained oxygen $2p$ levels 6 eV below the highest occupied level, and an equilibrium Fe-O interlayer spacing of 0.48 Å, when the oxygen was placed in the fourfold hollow site. Ribarsky, in an unrestricted Hartree-Fock cluster calculation,[7] predicted a vertical spacing of 0.38 Å. In recent $X\alpha$ cluster calculations,[8] Adachi et al. used a nine-atom substrate to study the level structure of O/Fe(001) versus the Fe—O bond site and bond length. For an interlayer spacing near 0.5 Å, three O $2p$ levels were obtained in the energy range 5 to 7 eV below E_F. The d-band density of states (DOS) was reduced near E_F due to the Fe-O interaction.

None of the calculations reviewed above included the

effects of adsorbate-adsorbate interactions in the extended O/Fe(001) system. This interaction broadens the O $2p$ levels, leading to two-dimensional energy bands. These bands hybridize at general points in the surface Brillouin zone (SBZ), but have definite reflection parity along the $\overline{\Sigma}$ and $\overline{\Delta}$ symmetry lines. They should be detectable using angle-resolved photoemission spectroscopy[9] (ARPES); the use of polarized light in conjunction with the selection rules[10] should aid in their identification.

Here we report calculations of the electronic structure of 1×1 O/Fe(001) using the self-consistent local orbital (SCLO) method.[11] Because this method incorporates an atomic-orbital basis, a simple picture of the surface bond can be developed from the numerical results. By treating electron-spin polarization explicitly,[12] we were able to study the magnetic behavior of this system as well as the influence of the magnetism on the bonding and energy-band structure. The SCLO method, the exchange-correlation potential, and the atomic geometry used in the calculations are described in the next section. The results are discussed in Sec. III.

II. METHOD

The SCLO method[11] expands the electronic wave function in atomic orbitals and computes matrix elements of the kinetic- and potential-energy operators by fitting the atomic orbitals to a set of Gaussian-type orbitals. While the starting potential is determined from overlapping free-atom charge densities, full self-consistency of the potential and charge density is developed in an iterative procedure in which potential variations are expanded in a Fourier series. Since no shape approximations are involved in the Fourier fit, the accuracy of the computed electronic structure is limited only by the basis-set flexibility and the local-density approximation[13,14] itself. Spin polarization can be included easily.[12]

Our basis set included all occupied atomic orbitals— oxygen $1s$, $2s$, and $2p$, and iron $1s$, $2s$, $2p$, $3s$, $3p$, $3d$, and $4s$—as well as a set of virtual orbitals on each atom to guarantee variational flexibility: oxygen $3s$ and $3p$, and iron $4p$ and $5s$. Trial calculations showed that virtual iron $4d$ states had a negligible effect on the electronic structure when added to the basis.

The exchange-correlation potential used was the one introduced in earlier studies of surface magnetism.[12,15] Essentially, it is a slightly modified form of the potential given by Vosko et al.,[16] who interpolated high-density electron-correlation energies (random-phase approximation) to low-density results[17] obtained in Monte Carlo calculations. The spin dependence of this potential differs slightly from that of von Barth and Hedin;[14] exchange splittings for a Ni(001) monolayer[12] are 2—8 % larger in the former potential, and the magnetic moment is larger by only 1%.

The charge and spin densities were determined at each step of iteration of the local-density equations by sampling the SBZ at six special points.[18] In the case of Ni(001) films,[15] on the other hand, our sampling included 15 special points, because of the high density of bands near E_F. Our calculations began with the paramagnetic

system, which was brought close to convergence before a trial exchange splitting was introduced to break the symmetry. We terminated the self-consistency cycles when all d-band matrix elements converged within 0.05 eV. Bandwidths, exchange splittings, and magnetic moments converged much more rapidly than did these matrix elements.

As in our earlier studies of surface electronic structure, we adopted a slab geometry to simulate the O/Fe(001) system. The five-layer metal substrate film had a geometry and interplanar spacing taken from the bulk, except that the outermost layers on both sides of the film were displaced 7.5% outward (1.54 Å compared with 1.43 Å). The oxygen atoms occupied all fourfold hollow sites on both sides of the substrate, with an Fe-O interlayer spacing of 0.48 Å. This structure was chosen to conform to the earlier LEED analysis.[1] The resulting Fe—O bond lengths of 2.08 and 2.02 Å (for first- and second-layer Fe atoms, respectively) imply an oxygen "radius" of 0.78 Å, somewhat larger than the covalent radius 0.66 Å, but close to the value 0.73 Å found in the $c(2 \times 2)$ O/Ni(001) system.[19] We did not include subsurface oxygen atoms, because so little is known about their incorporation[1-5] in the relevant exposure range ~ 6 L. Because the surface perturbation is healed within the first few layers on transition-metal substrates, we feel our seven-plane slab model should provide a reliable account of the surface bond and well-localized surface interface states. Indeed, essentially the bulk electronic structure[20] is observed at the central layer of the slab.

III. RESULTS

A. Charge and spin densities

The self-consistent charge and spin densities are shown in Figs. 1 and 2. Charge-density contours differing by the
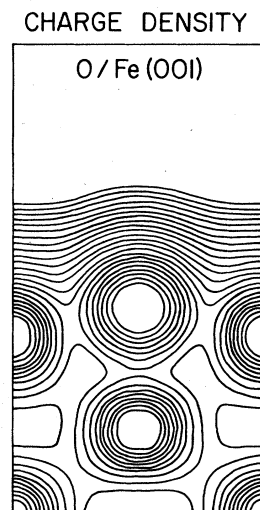
CHARGE DENSITY

FIG. 1. Charge-density contours in the (110) plane normal to the surface of the O/Fe$_5$(001) slab. Contour values increase by the factor 1.414 as the core region is approached. The oxygen atoms were positioned in the fourfold hollows of the metal surface, at a distance 0.48 Å above the surface plane.
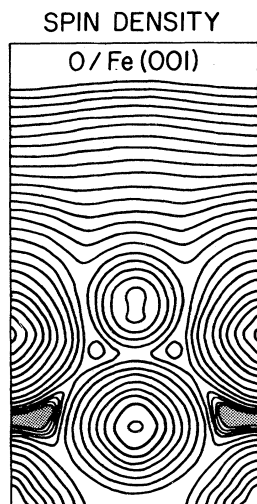
SPIN DENSITY

FIG. 2. Spin-density contours for O/Fe(001), plotted in the (110) plane. Successive contours have the ratio 2, increasing toward the nuclei. Weak negative magnetization is indicated by the shading.

ratio 1.414 are drawn in a (110) plane normal to the surface; spin-density contours differing by a factor of 2 are also given. Note that these figures have a bulklike appearance below the Fe-O interface. At the interface, covalent bonds between oxygen and Fe atoms in the first and second metal layers are evident in the buildup of charge along the internuclear axes. Because the oxygen layer is located deep within the metal surface, a definite smoothing of the charge-density corrugation is obtained in the vacuum region. The atomic orbitals most prominent in forming the surface bonds will be discussed later. The spin density, Fig. 2, is also smoothed by the oxygen, which itself acquires a small magnetization. The adsorption does not quench the surface magnetism of the substrate, although the "eruptions" into vacuum noted on the clean surface[21] are absent. Some weak, negative magnetization is found between neighboring Fe atoms.

B. Densities of states (DOS's)

The nature of the surface chemical bond is easily clarified by examining layer-projected DOS's given in Figs. 3 and 4. These were obtained by interpolating energies calculated at 45 points in the irreducible SBZ to 20 000 randomly generated points. Histograms generated by counting levels in 75-meV-wide channels were smoothed by five-point averaging to reduce statistical noise. Each level was weighted according to its occupation probability on (Löwdin-orthogonalized) layer orbitals. The DOS's are given in Fig. 3, together with those of the clean-metal slab for comparison. The DOS of the oxygen layer has pronounced features in a 4-eV-wide distribution centered 5.5 eV below E_F.

In addition to the bonding levels below the $3d$ bands in Fig. 3, the adlayer DOS has a broad band of antibonding levels that extend about 2 eV above E_F. The unoccupied portion of these bands serve as final states for electrons
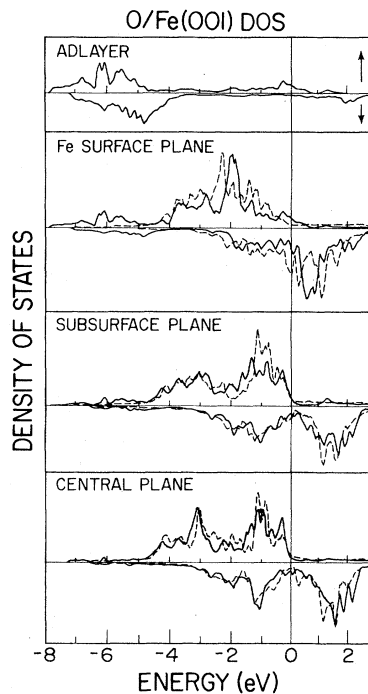
O/Fe(OOI) DOS

FIG. 3. Layer-resolved DOS's of O/Fe(001). E_F is the energy zero. The vertical scale is arbitrary. Statistical noise has been suppressed by five-point averaging. Majority- (minority-) spin DOS's are indicated by ↑(↓). Results obtained for the clean Fe(001) film (shifted to align E_F) are shown with dashed lines.

excited from the bonding $2p$ band by EELS;[2] a prominent transition is observed near 6 eV. Appearance potential spectroscopy (APS) measurements[22] have also identified an empty band of oxygenlike states about 1 eV above E_F. Note that while the oxygen-layer DOS is weak in the occupied $3d$-band region, Fe-O mixing is not negligible: the surface (S) and subsurface $(S-1)$ Fe DOS's have significant amplitude in the O $2p$ region.

Oxygen adsorption substantially narrows the DOS of the Fe(001) surface, as seen in Fig. 3; the main majority-spin peak is located about 2.0 eV below E_F. As shown below, this peak has largely Fe $3d_{z^2}$ character. The DOS's of deeper layers have a bulklike appearance, except for the weak O $2p$ bands below -4 eV. The amplitude of layer-projected DOS's in the O $2p$ region, and the reduction of d-band amplitude, are directly correlated with the strength of Fe-O hybridization. As expected, the O $2p$ peaks are very weak in the film center. Hybridization is not negligible for subsurface Fe atoms, however, since oxygen adatoms are in close proximity to them. Note that the Fe—O bond length[1] is actually smaller for the second plane, 2.02 Å, than for the first plane, where it is 2.08 Å.

The planar DOS's in Fig. 3 can be resolved into atomic-orbital components for further insight concerning the surface bond. We present Fe $3d$ and O $2p$ DOS's in Fig. 4. We begin with the top-layer-Fe DOS's in Fig. 4(a). Among the $3d$ orbitals, both $3z^2-r^2$ and x^2-y^2 have strong, narrow DOS peaks about 1.5 eV below E_F for majority spin; compare Fig. 3. Only very weak O $2p$ hybridization occurs for the $3z^2-r^2$ orbital, presumably because
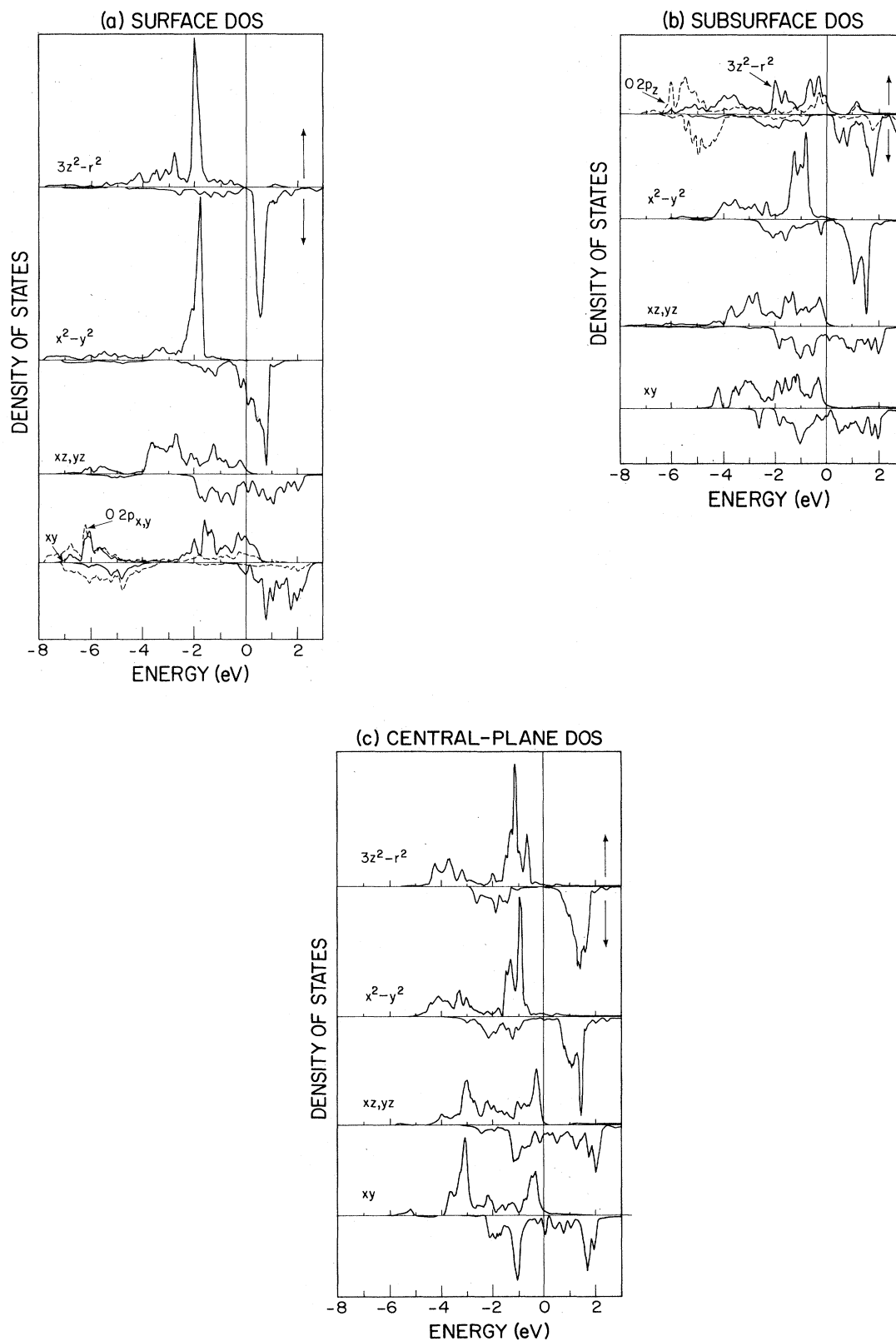
FIG. 4. Fe $3d$—orbital DOS's of O/Fe(001), for (a) the surface plane, (b) the subsurface plane, and (c) the center plane of the metal substrate. For comparison purposes, the O $2p$—orbital DOS's are also shown; the $2p_x$ ($2p_y$) DOS is superimposed on the surface-layer $3d_{xy}$ DOS, and the $2p_z$ DOS on the subsurface $3d_{3z^2-r^2}$ DOS. The $2p$ DOS's are shown as dashed lines.

of its vertical orientation, which minimizes its interaction with oxygen atoms positioned in hollow sites. The xz and yz orbitals (equivalent by symmetry) have somewhat stronger interaction with oxygen, but certainly do not dominate the bonding as suggested earlier.[2] Instead, it is the planar orbitals, of x^2-y^2 and xy character, that have the strongest hybridization with oxygen, and hence the largest DOS peaks below the d bands. This result is consistent with the nearly coplanar geometry assumed in the calculations. In particular, the xy orbital, with lobes directed into the fourfold hollow sites, has the strongest hybridization with O $2p$ levels. Note the intense DOS structure below -4 eV, as well as the strong repulsion of $3d_{xy}$ levels toward higher energies. Also, because the shape of the xy DOS in the O $2p$ region is so similar to that of the $2p_x, 2p_y$ band of the adlayer, we conclude that the primary bonding mechanism is Fe d_{xy}—O p_x, p_y. Again, geometrical considerations suggest that the p_z orbital should play a minor role.

Now consider the orbital DOS's of the second Fe layer. In this case, as seen in Fig. 4(b), only the $3z^2$-r^2 DOS has a sizable amplitude below -4 eV. Moreover, the DOS shape there resembles the O $2p_z$ and not the O $2p_x$-$2p_y$ band on the adlayer. We may infer that oxygen bonds to subsurface Fe atoms according to the scheme Fe $d_{3z^2\text{-}r^2}$—O p_z. This mechanism is understandable considering the vertical relationship of the two atoms.

Finally, Fig. 4(c) shows that oxygen hybridizes very little with Fe orbitals at the slab center. Although a slightly thicker slab would be required to completely eliminate hybridization at the center, our slab is sufficiently thick to provide nearly bulklike electronic structure at the central plane (compare Fig. 3) and to reduce the interaction between opposite interfaces.

C. Atomic-orbital occupancies

Occupation numbers in the Löwdin basis[15,23] of orthogonalized atomic orbitals are given in Tables I and II. The d-orbital occupancies, Table I, are affected by both the surface potential and the oxygen adlayer. At the surface of the clean film, all d-orbital occupation numbers are slightly larger than their central-plane values except for the xz and yz orbitals; the central-plane results should be representative of the bulk. The surface-induced increase

is due to dehybridization:[15] *nominal* d-band levels have higher d character at the surface. Because the various d orbitals on a given atom have very similar occupancies, the charge density is nearly isotropic in the d shell; see Fig. 1. On the other hand, the spin density shown in Fig. 2 is anisotropic, reflecting the dominance of e_g ($3z^2$-r^2, x^2-y^2) orbitals.

Oxygen adsorption perturbs the metal d-orbital occupancies, especially those involved in the Fe—O bonding. Within the (metal) surface plane, the xy occupation number is reduced from 1.40 to 1.09 electrons per atom, while the surface $3z^2$-r^2 electron count falls from 1.31 to 1.21 when oxygen is present. Both decreases are due to O $2p$—Fe $3d$ level repulsion and a transfer of d character into antibonding levels above E_F. The nonbonding x^2-y^2 orbital experiences almost no oxygen-induced changes of occupation. Finally, the surface xy (or yz) occupancy increases from 1.38 to 1.47 electrons per atom when oxygen is adsorbed. The total number of atomic d electrons n_d is reduced by 0.26, 0.02, and 0.12 on surface, subsurface, and central planes of the oxygenated film, respectively.

Surface and oxygen-induced charge transfer can be studied using the results in Table II. In addition to the changes in n_d noted above, results for n_{sp} and the total valence occupation $n = n_d + n_{sp}$ are given. While the clean metal film exhibits charge neutrality (eight valence electrons per atom) to within 0.03 electron per atom, oxygen attracts a significant number of electrons from the surface and subsurface layers. In particular, 0.63 electrons are transferred from the metal to each oxygen atom, leaving behind a charge deficit of 0.52, 0.05, and 0.11 on planes S, $S - 1$, and C, respectively. These numbers are subject to the caveat that Löwdin basis functions[23] have somewhat longer range than conventional atomic orbitals, due to their orthogonality, leading to a tendency for the surface charge deficit to be partly assigned to interior planes. In any case, such a larger transfer of charge is not unreasonable, given the huge electronegativity of oxygen, which is often assigned a formal charge of two electrons in compound formation. One expects a large work-function shift due to the dipole layer created at the interface. We found the value $\Delta\phi = 1.4$ eV; the work function we calculated for Fe$_5$ is 4.4 eV, in excellent agreement with the experimental value.[24] Observed values[2,4,5] of $\Delta\phi$

TABLE I. d-orbital occupation numbers per atom for a clean five-plane Fe(001) film, Fe$_5$, and five-plane film with oxygen atoms positioned in the fourfold hollow sites on both faces, O/Fe$_5$. The geometry is described in the text. The iron surface, subsurface, and center planes are labeled S, $S - 1$, and C. n_d is the total number of d electrons per atom.

Film	Layer	Atomic orbital				
		$3z^2$-r^2	x^2-y^2	xz or yz	xy	n_d
Fe$_5$	S	1.31	1.31	1.38	1.41	6.80
	$S - 1$	1.28	1.22	1.42	1.40	6.74
	C	1.27	1.29	1.41	1.35	6.74
O/Fe$_5$	S	1.21	1.31	1.47	1.09	6.54
	$S - 1$	1.21	1.27	1.43	1.43	6.72
	C	1.21	1.28	1.35	1.42	6.62

TABLE II. Occupation numbers and magnetic moments per atom for Fe$_5$ and O/Fe$_5$ films. A denotes the oxygen adsorbate layer. n_d and n_{sp} are the atomic d- and sp-shell occupancies, $n = n_d + n_{sp}$, and m is the magnetic moment per atom. Values of n obtained by other workers (Ref. 26) for Fe$_5$ are given in parentheses in the last column.

Film	Layer	n_d	n_{sp}	n	$m (\mu_B)$
Fe$_5$	S	6.80	1.23	8.03	2.89 (2.94)
	$S-1$	6.74	1.25	7.99	2.31 (2.32)
	C	6.74	1.23	7.97	2.49 (2.52)
O/Fe$_5$	A		6.63	6.63	0.24
	S	6.54	0.94	7.48	2.93
	$S-1$	6.72	1.23	7.95	2.52
	C	6.62	1.27	7.89	2.68

for O/Fe(001) in the chemisorption stage are generally less than 0.4 eV, perhaps due to the incorporation of oxygen into the selvedge region.

D. Magnetism

Recent spin-resolved photoemission experiments[25] suggest that oxygen removes the surface magnetism of Ni(110), while it has only slight influence on the magnetism of an Fe-based glass. Our results for the layer-resolved (Löwdin projections[23]) magnetic behavior of O/Fe (001) and clean Fe(001) are given in the last column of Table II together with results obtained earlier by Ohnishi et al.[26] Note the substantial surface enhancement of the magnetic moment of the clean metal film (16% compared with the center-plane value). This enhancement is not removed by the adsorbed oxygen; the magnetic moment per atom, m, increases slightly, from 2.89μ_B to 2.93μ_B. Thus oxygen adsorption does not produce "dead layers". The oxygen adlayer is spin polarized, with a magnetic moment of 0.24μ_B per atom, about 8% of the value on a surface Fe atom.

E. Surface-state bands

To determine surface bands on O/Fe(001), we selected states in the SBZ which had more than 60% occupation probability on the Fe-O bilayer. These states were divided further into "weak" and "strong" surface states, the latter having Fe-O occupation greater than 80%. These bands are shown Fig. 5. As expected, strong surface bands are found in the range 4 to 8 eV below E_F, i.e., just below the Fe 3d bands. These oxygenlike bands may be described as bonding levels, and disperse as simple tight-binding energy bands based on p orbitals. There are two sets of p bands for each spin direction corresponding to symmetric [Fig. 5(a)] and antisymmetric [Fig. 5(b)] combinations of bonding levels on the two equivalent faces of the slab.
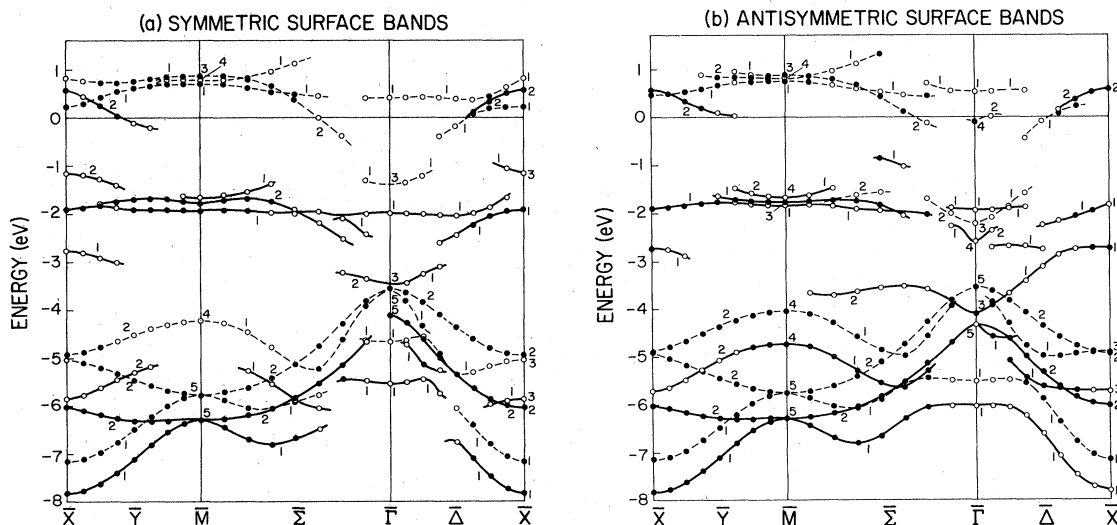

FIG. 5. Spin-split surface bands of O/Fe(001), defined as energy bands with more than 60% localization on the Fe-O bilayer. Strong surface states, labeled with solid circles, have more than 80% Fe-O interface character, weak states (open circles) less than 80%. Majority- (minority-) spin bands are indicated with solid (dashed) lines. E_F is the energy zero. Along the symmetry lines $\overline{Y}$, $\overline{\Sigma}$, and $\overline{\Delta}$, bands labeled 1 are even with respect to the appropriate vertical mirror plane; those labeled with 2 are odd. The states are further separated into levels which are (a) symmetric and (b) antisymmetric with respect to the horizontal mirror plane in the film center. These levels would be degenerate for a very thick film.

The energy splitting is a measure of the interaction between the faces, and would vanish for a thick slab. In these figures, the p_z band extends as follows: $\overline{X}_3\overline{M}_4\overline{\Gamma}_1\overline{X}_3$; it hybridizes with the p_x (p_y) band along $\overline{\Delta}$ ($\overline{Y}$). The p_x and p_y bands are degenerate at $\overline{M}_5$ and $\overline{\Gamma}_5$, with p_x being lower along $\overline{Y}$ and $\overline{\Delta}$. The p_z band hybridizes with the even band p_{x+y} along $\overline{\Sigma}$. Exchange splittings in the O $2p$ bands vary from 0.5 to 1.0 eV.

The oxygen-induced bands 4 to 8 eV below E_F should be resolvable using ARPES.[9] Their energetic separation from the bulk Fe levels and their relatively flat dispersion make them good candidates for observation. The use of polarized light together with the selection rules[10] for ARPES would facilitate the identification of bands along the $\overline{\Delta}$ and $\overline{\Sigma}$ lines, which contain mirror planes. In particular, even bands labeled $\overline{\Delta}_1$ and $\overline{\Sigma}_1$ are excited by light polarized in the respective mirror planes, while the odd bands, $\overline{\Delta}_2$ and $\overline{\Sigma}_2$, require a component of the vector potential perpendicular to these planes. A broad oxygen-induced resonance was observed 5.5 eV below E_F in angle-integrated photoemission data.[4,5]

A second set of surface bands is also seen in Fig. 5. These are located in the Fe $3d$ bulk continuum, and have higher Fe character than the bands just discussed. Because of their large Fe amplitudes, the bands have large exchange splittings; the actual values depend on the degree of surface localization as well as the Fe character. In comparison with clean Fe(001),[21] the oxygenated surface has fewer surface-state bands in the $3d$ region. The greatest concentration is found 1 to 2 eV below E_F (we discuss only majority-spin bands). An $\overline{X}_1\overline{Y}_1\overline{M}_1\overline{\Sigma}_1$ band is particularly prominent; it is quite flat, is centered near -1.5 eV, and has mainly $3z^2-r^2$ character. One expects this band to be only weakly affected by oxygen atoms located in fourfold hollow sites. An x^2-y^2 surface band $\overline{Y}_1\overline{M}_3\overline{\Sigma}_2$ is also "strong;" it is centered near -1.2 eV. Weak bands are found near $\overline{M}_4$ (xy character), $\overline{\Gamma}_3$ (xy) near the d-band edge, and along $\overline{\Delta}_1$ near $\overline{X}_1$ ($3z^2-r^2, x^2-y^2$). Some of the "weak" surface states may convert to bulk states in thicker slabs.

ACKNOWLEDGMENTS

[1]K. O. Legg, F. Jona D. W. Jepsen, and P. M. Marcus, Phys. Rev. B 16, (1977); J. Phys. C 8, L492 (1975).

[2]Y. Sakisaka, T. Miyano, and M. Onchi, Phys. Rev. B 30, 6849 (1984).

[3]G. W. Simmons and D. J. Dwyer, Surf. Sci. 48, 373 (1975).

[4]C. Brucker and T. N. Rhodin, Surf. Sci. 57, 523 (1976).

[5]K. Y. Yu, W. E. Spicer, I. Lindau, P. Pianetta, and S. F. Lin, Surf. Sci. 57, 157 (1976).

[6]A. B. Anderson, Phys. Rev. B 16, 900 (1977).

[7]M. W. Ribarsky, Solid State Commun. 38, 935 (1981).

[8]H. Adachi, M. Tsukada, I. Yasumori, and M. Onchi, Surf. Sci. 119, 10 (1982).

[9]A. M. Turner and J. L. Erskine, Phys. Rev. B 30, 2377 (1984).

[10]J. Hermanson, Solid State Commun. 22, 9 (1977).

[11]J. R. Smith, J. G. Gay, and F. J. Arlinghaus, Phys. Rev. B 21, 2201 (1980).

[12]X.-Y. Zhu and J. Hermanson, Phys. Rev. B 27, 2092 (1983).

[13]W. Kohn and L. J. Sham, Phys. Rev. 140, A1133 (1965).

[14]U. von Barth and L. Hedin, J. Phys. C 5, 1629 (1972).

[15]X.-Y. Zhu, J. Hermanson, F. J. Arlinghaus, J. G. Gay, R. Richter, and J. R. Smith, Phys. Rev. B 29, 4426 (1984).

[16]S. H. Vosko, L. Wilk, and M. Nusair, Can. J. Phys. 58, 1200 (1980).

[17]D. M. Ceperley and B. J. Alder, Phys. Rev. Lett. 45, 566 (1980).

[18]S. J. Cunningham, Phys. Rev. B 10, 4988 (1974).

[19]J. E. Demuth, D. W. Jepsen, and P. M. Marcus, Phys. Rev. Lett. 32, 540 (1973).

[20]V. L. Moruzzi, J. F. Janak, and A. R. Williams, Calculated Electronic Properties of Metals (Pergamon, New York, 1978).

[21]S. Ohnishi, A. J. Freeman, and M. Weinert, Phys. Rev. B 28, 6741 (1983).

[22]S. Andersson and C. Nyberg, Surf. Sci. 52, 489 (1975).

[23]P. O. Löwdin, J. Chem. Phys. 18, 365 (1950).

[24]A. M. Turner, Yu. J. Chang, and J. L. Erskine, Phys. Rev. Lett. 48, 348 (1982).

[25]W. Schmitt, H. Hopster, and G. Güntherodt, Phys. Rev. B 31, 4035 (1985).

[26]S. Ohnishi, M. Weinert, and A. J. Freeman, Phys. Rev. B 30, 36 (1984).